ORIGINAL ARTICLE
Iran J AllergyAsthmaImmunol
August 2026; 25(4):583-593.
DOI: 10.18502/ijaai.v25i4.21744

Effects of a CB2 Receptor Inverse Agonist on Airway Remodeling and T_H1/T_H2 Imbalance in Rats with Bronchial Asthma via the TLR4/NF-κB Signaling Pathway

Wen Zhou[1] and Jinping Gao[2]

[1] Department of Respiratory Asthma, Xi'an Qidi Children's Hospital, Xi'an, Shaanxi, China
[2] Department of Integrated Traditional Chinese and Western Medicine, Xi'an Qidi Children's Hospital, Xi'an, Shaanxi, China

Received: 30 March 2025; Received in revised form: 13 May 2025; Accepted: 12 June 2025

ABSTRACT

Bronchial asthma (BA) has a complex pathogenesis involving immune imbalance and airway remodeling (AR). Cannabinoid receptor 2 (CB2) plays a role in inflammation regulation, so this study explored the therapeutic potential of a CB2 inverse agonist on BA rats' AR and Th1/Th2 imbalance, and its mechanism via Toll-like receptor 4/nuclear factor kappa B(*TLR4/NF-κB*) pathway.

Twenty-seven male SD rats (180-220 g) were divided into control (CG), model (MG), and intervention (IG) groups (n=9 each). MG/IG were BA-modeled by ovalbumin (OVA) sensitization (days 1/8: 100 μg OVA +1 mg aluminum hydroxide gel, i.p.) and 1% OVA aerosol challenge (day 15, 3×/week, 8 weeks). IG received CB2 inverse agonist (5 mg/kg, i.p., 3×/week, 4 weeks); CG/MG got saline. T_H1/T_H2 cytokines, subsets, AR parameters, and lung *TLR4/NF-κB*-related molecules were detected.

Compared with CG, MG had T_H1/T_H2 imbalance, higher AR indices, upregulated *TLR4/NF-κB*, shorter asthma latency, and longer attack duration. vs. MG, IG reversed T_H1/T_H2 imbalance, reduced *TLR4/NF-κB*-related protein/mRNA (except elevated *NFKBIA*).

CB2 inverse agonist has BA prevention/treatment potential by regulating Th1/Th2 balance, inhibiting AR, and acting on the *TLR4/NF-κB* pathway.

Keywords: Airway remodeling; Bronchial asthma; CB2 receptor inverse agonist; Immune imbalance; TLR4/NF-κB pathway

INTRODUCTION

Bronchial asthma (BA), a global health issue, poses a serious threat to human respiratory health. Its incidence has been rising continuously over the past decades, becoming a significant public health concern.[1] Asthma is a chronic inflammatory airway disease that involves multiple cell types (eg, eosinophils) and cellular components that contribute to the inflammatory process.[2,3] Clinically, patients often experience symptoms such as wheezing, shortness of breath, chest tightness, or cough, which are often exacerbated at night and in the early morning.[4] These symptoms not only

Corresponding Author: Jinping Gao, MD;
Department of Integrated Traditional Chinese and Western Medicine, Xi'an Qidi Children's Hospital, Xi'an, Shaanxi, China. Tel: (+86-151) 0127 7712, Fax: (+86 029) 8862 9999, Email: 15101277712@163.com

affect daily activities, such as reducing exercise tolerance and severely decreasing sleep quality, but can also be life-threatening during acute exacerbations if not promptly treated. Airway remodeling (AR) involves a series of complex changes, including airway smooth muscle proliferation, increased deposition of extracellular matrix, and subepithelial fibrosis, which severely impair airway function and are key factors leading to persistent and recurrent asthma.[5]

Immune system imbalance plays a central role in driving asthma pathogenesis. T_H2 cells become overactivated, secreting large amounts of cytokines such as interleukin (IL)-4, which promote eosinophil infiltration and increased mucus secretion, further exacerbating airway inflammation and remodeling.[6] In contrast, T_H1 cell-related cytokines like interferon (IFN)-γ are relatively insufficient, failing to effectively counterbalance the T_H2 dominance and causing a continuous tilt in the immune balance.[7]

In the field of asthma treatment, researchers are exploring more precise and effective intervention targets and strategies. In recent years, the endocannabinoid system (ECS) has become a focus of research, with the cannabinoid receptor 2 (CB2) emerging as a promising therapeutic target.[8–10] Activation of CB2 receptors can initiate a series of intracellular signal transductions, demonstrating strong anti-inflammatory potential and opening new avenues for asthma treatment.[11] In contrast to traditional treatments, targeting CB2 receptors has the potential to directly address the underlying inflammation in asthma and regulate the immune microenvironment. However, most current studies focus on conventional CB2 receptor agonists, which, while able to alleviate asthma symptoms to some extent, have limitations such as the development of tolerance and uncontrollable adverse reactions with long-term use.[12] In contrast, inverse agonists, as a new class of regulators, have a unique mode of action. Instead of simply mimicking the activation of receptors by endogenous ligands, they stabilize the inactive conformation of receptors, reverse their intrinsic activity, and thereby regulate downstream signals. Theoretically, they may avoid some of the drawbacks of traditional agonists and bring new opportunities for asthma treatment.[13,14]

This study explores the mechanisms of a CB2 receptor inverse agonist in a rat model of BA. It specifically investigates how the agonist mediates the Toll-like receptor 4 (TLR4)/nuclear factor-κB (NF-κB) pathway and provides a detailed analysis of its effects on AR. The aim was to clarify whether a CB2 receptor inverse agonist can precisely regulate key signaling hubs, reshape immune balance, and inhibit the AR process, providing new theoretical support and potential drug targets for future clinical asthma treatment. This study may help fill a gap in current asthma precision treatment strategies and reduce disease severity.

MATERIALS AND METHODS

Experimental Animals

Twenty-seven male Sprague-Dawley rats (weight, 180–220 g), certified specific pathogen-free, were procured from Jiangsu Ailingfei Biotechnology Co., Ltd. Upon arrival, the animals were allowed to acclimatize to the new environment in a controlled barrier facility. This facility was maintained at a constant temperature of 22 ± 2°C and a relative humidity of 50% to 60%, ensuring optimal conditions for the animals' well-being. Additionally, the facility operated on a strict 12-hour light/dark cycle to simulate natural day and night conditions, further promoting the animals' comfort and reducing stress during the acclimatization period. Throughout the acclimation period, the rats were provided *ad libitum* access to standard rodent chow and water to ensure environmental adaptation and minimize stress-related variables that could potentially influence experimental outcomes. The principles of replacement, reduction, and refinement (the 3Rs) were always upheld to minimize animal suffering and optimize experimental procedures. The experimental staff regularly monitored the rats' general condition, including their mental state, feeding, and excretion. Any abnormalities were promptly addressed to ensure that the rats completed the experimental period in a relatively comfortable state, thereby providing a reliable and stable data foundation for subsequent research. All experiments strictly complied with the Guide for the Care and Use of Laboratory Animals (National Institutes of Health publication 80-23, revised 1978).

Animal Grouping and Model Preparation

The 27 rats were randomly allocated to 3 groups (n=9 each): a control group (CG), a model group (MG), and an intervention group (IG). The CG consisted of normal rats, while the MG and IG were prepared as BA models. The model preparation was carried out using the classic ovalbumin (OVA) sensitization and provocation method: on days 1 and 8 of the experiment, the MG and IG were

Published by Tehran University of Medical Sciences (http://ijaai.tums.ac.ir)

given an intraperitoneal injection of 1 mL of a saline suspension containing 100 μg of OVA and 1 mg of aluminum hydroxide gel (Jiangsu Baoyi Pharmaceutical Co, Ltd) for sensitization. Starting on day 15 of the experiment, the rats were placed in a closed acrylic nebulization chamber and exposed to nebulized 1% OVA saline solution for 30 minutes, 3 times a week, for 8 weeks. During this time, the rats' respiratory rate, amplitude, and overall condition were closely monitored. If severe allergic reactions, such as rapid breathing or cyanosis, occurred, nebulization was immediately halted, and appropriate emergency measures were implemented to ensure the rats' safety and the success and stability of the model. This approach laid the foundation for subsequent research on BA-related pathophysiological changes and intervention effects.

Intervention Method

After the OVA sensitization and provocation operations were completed and the asthma models in the MG and IG were confirmed to be successfully established, the IG began treatment with a CB2 receptor inverse agonist. Based on preliminary experiments and relevant literature, the drug dose was determined to be 5 mg/kg. The drug was dissolved in sterile saline to ensure its stability and uniformity for intraperitoneal injection. The CG and MG received an equal volume of saline via intraperitoneal injection. During the injection procedure, the experimental staff used a 1-mL syringe with a 25-G needle. The rat was gently restrained, and the needle was inserted into the lower abdomen on the lateral side. The drug was then slowly injected to avoid damage to the abdominal organs and to ensure accurate delivery into the peritoneal cavity. Injections were administered 3 times a week for 4 weeks to fully maximize the inverse agonist effect of the drug on CB2 receptors. Throughout the intervention period, the rats' general condition, feeding and drinking, and any potential adverse drug reactions were continuously and closely monitored. If the rats exhibited abnormal signs such as lethargy, diarrhea, or sudden weight loss, the latency to asthma induction and the total duration of asthma attacks (tAAD) were promptly recorded, and the dosing regimen was adjusted if necessary to ensure the smooth progress of the experiment.

Enzyme-Linked Immunosorbent Assay (ELISA)

In this study, the levels of T_H1/T_H2 cytokines (eg, IFN-γ, IL-4) in bronchoalveolar lavage fluid were measured using the ELISA method. The experimental procedure was as follows: at the end of the experiment, rats were deeply anesthetized and intubated (Hangzhou Bofei Medical Instrument Co, Ltd). Bronchoalveolar lavage was performed with precooled sterile physiological saline (approximately 1 mL per wash, repeated 3 times). After collection, the lavage fluid was centrifuged at 1000 rpm for 10 minutes at 4°C, and the supernatant was stored at −80°C for future use. The ELISA kit from Keluo (Wuhan) Biotechnology Co, Ltd, was used, and the assay was conducted strictly according to the manufacturer's instructions: reagents were equilibrated at 25°C for 30 minutes, and the standard curve working solution was prepared. In a 96-well plate, 100 μL of standard or sample (in triplicate) was added to each well and incubated at 25 °C for 2 hours. After washing the plate 3 times, 100 μL of enzyme-labeled antibody working solution was added and incubated at 25°C for 1 hour. Following a second wash, 100 μL of substrate solution was added, and the reaction was carried out in the dark for 15 to 30 minutes. The reaction was then stopped by adding 50 μL of stop solution, and the optical density (OD) value was measured at 450 nm. The concentrations of the cytokines were calculated using the standard curve, and quality control samples were included throughout the experiment to ensure data reliability.

Flow Cytometry

The proportion of T_H1/T_H2 cell subsets in the spleen was detected using flow cytometry (Beijing Cenglang Biological Technology Co, Ltd). The main steps were as follows: under sterile conditions, a single-cell suspension from the spleen was prepared by filtering through a 200-mesh filter (Beijing Solarbio Technology Co, Ltd), followed by red blood cell lysis. The cell density was then adjusted to 1×10^6 to 1×10^7 cells/mL. Fluorescently labeled antibodies, CD4-FITC and IFN-γ-PE (for T_H1 cells) and CD4-FITC and IL-4-APC (for T_H2 cells), were added and incubated in the dark at 4°C for 30 minutes. After washing with phosphate-buffered saline (PBS), the samples were analyzed using a flow cytometer. Lymphocyte populations were first gated based on the forward scatter/side scatter (FSC/SSC) plot, and the proportion of $CD4^+IFN\text{-}\gamma^+$ (T_H1) and $CD4^+IL\text{-}4^+$ (T_H2) cells was determined. Data were analyzed using FlowJo software, with at least10 000 cell events per sample analyzed per group.

Measurement of AR Morphological Parameters

After fixation in 4% paraformaldehyde for 24 hours, lung tissues were subjected to graded ethanol dehydration, xylene (Shanghai Bailihui Chemical Technology Co, Ltd) clearing, and paraffin embedding. Continuous sections of 5-μm thickness were prepared and stained with hematoxylin-eosin (HE) (hematoxylin for 5 minutes, eosin for 3 minutes). The sections were then observed under an optical microscope (Leica Microsystems [Shanghai] Trading Co, Ltd). The following parameters were measured: bronchial basement membrane perimeter (Pbm), total wall area (wAt), inner wall area (wAi), and smooth muscle wall area (wAm). Standardized parameters were calculated using Image-Pro Plus software: wAt/Pbm (total wall thickness), wAi/Pbm (inner wall thickness), and wAm/Pbm (smooth muscle layer thickness). At least 5 airway cross-sections of similar size were randomly measured per group.

Western Blot Analysis

Western blot analysis was used to detect the protein expression of TLR4, NF-κB, and its downstream key molecules (MyD88, IκBα, p-IκBα) in rat lung tissue. The experiment employed a Western blot detection kit from Wuhan Newlai Biotechnology Co, Ltd. The procedure was as follows: frozen tissue samples stored at −80 °C were lysed using RIPA buffer containing protease inhibitors (Wuhan Newlai), and total protein was extracted. Protein concentration was determined using a BCA protein assay kit. After performing 10% sodium dodecyl sulfate–polyacrylamide gel electrophoresis (SDS-PAGE) (30 μg per well) and transferring to a polyvinylidene fluoride (PVDF) membrane, the membrane was blocked with 5% nonfat milk for 1 hour. Primary antibodies, including TLR4 (1:1000) and NF-κB p65 (1:800), were incubated overnight at 4 °C. Following membrane washing with TBST, horseradish peroxidase (HRP)–conjugated secondary antibody (1:5000) was added and incubated at room temperature for 1 hour. Enhanced chemiluminescence (ECL) detection was performed, and protein bands were analyzed using ImageJ software. The relative expression levels were calculated by normalizing to β-actin, and the differences between groups were compared.

Quantitative Polymerase Chain Reaction (qPCR) Analysis

Real-time qPCR was employed to detect the Mrna expression of key molecules in the TLR4/NF-κB signaling pathway (*TLR4*, *MyD88*, *NF-κB p65*) and its regulatory factor *IκBα* in lung tissue. The qPCR detection kit was purchased from Nanjing Novogene Bioinformatics Technology Co, Ltd. The same batch of frozen tissue used in the Western blot experiment was used to ensure consistency of experimental samples. Total RNA was extracted using the TRIzol method, and cDNA was synthesized using the PrimeScript RT reagent kit. Amplification was performed with TB Green Premix Ex Taq II (Takara), and the primers used were as follows:

TLR4 (F: 5'-GCTGGCTTAATTACCCGT-3', R: 5'-TCCAGGTAGGTCTTGGTCT-3');

MyD88 (F: 5'-AGTGTTCGGGACTTCGTG-3', R: 5'-GTAGGCGATCTCGTAGTTG-3');

NF-κB p65 (F: 5'-CAGAGGGACTACGTGCGAT-3', R: 5'-GGATGCGTTTCCGTAGAGG-3');

IκBα (F: 5'-GATGACCGAGTACCTGAACG-3', R: 5'-TCCTTGCTGATCTCGATGTC-3').

Note: Under standard qPCR conditions, the same primer pair cannot specifically amplify two distinct genes (except for rare cases of highly conserved homologous genes with identical primer-binding sites, which is not applicable to the above genes). The primer sequences for each target gene were designed based on their unique coding sequences and verified for specificity via BLAST (Basic Local Alignment Search Tool) to avoid non-specific amplification. β-actin was used as an internal reference gene. The relative expression levels were calculated using the $2^{-\Delta\Delta Ct}$ method.

Statistical Analysis

Data were analyzed using SPSS software (version 22.0; IBM Corp). Normally distributed measurement data were represented as mean (SD), and no categorical data (e.g., binary or nominal variables) were involved in this study. For measurement data that did not follow a normal distribution, the Kruskal-Wallis H test (a non-parametric test suitable for comparing three or more independent groups) was adopted for overall comparisons among the three groups (control group [CG], model group [MG], intervention group [IG]); if a significant overall difference was detected, pairwise comparisons were performed using the Mann-Whitney U test (with Bonferroni correction to adjust for type I error). For normally distributed measurement data, 1-way analysis of variance (ANOVA) was adopted for

overall comparisons among the three groups; if ANOVA indicated a significant overall difference, pairwise comparisons were conducted using post-hoc tests (e.g., LSD or Tukey's HSD). A 2-sided p<0.05 was considered statistically significant.

RESULTS

T_H1/T_H2 Cytokine Levels in the Bronchoalveolar Lavage Fluid of the 3 Groups of Rats

As shown in Figure 1, compared with the CG, the MG and IG had elevated levels of IL-4 and IL-5 and lower levels of IL-12 and IFN-γ. Compared with theMG, the IG had lower levels of IL-4 and IL-5 and higher levels of IL-12 and IFN-γ (p<0.05 for all comparisons).

Comparison of T_H1/T_H2 Cell Subsets Among the 3 Groups of Rats

As shown in Figure 2, compared with the CG, the MG and IG had a lower proportion of $CD4^+IFN\text{-}\gamma^+$ cells and a lower T_H1/T_H2 ratio, while the proportion of $CD4^+IL\text{-}4^+$ cells was higher. Compared with the MG, the IG had a higher proportion of $CD4^+IFN\text{-}\gamma^+$ cells and a higher T_H1/T_H2 ratio, and the proportion of $CD4^+IL\text{-}4^+$ cells was lower (p<0.05 for all comparisons).

Comparison of AR Morphological Parameters Among the 3 Groups of Rats

As shown in Figures 3 and 4, compared with the CG, the MG and IG had higher wAt/Pbm, wAm/Pbm, and wAi/Pbm values. Compared with the MG, these values were lower in the IG (p<0.05 for all comparisons).

Comparison of Protein Expression of TLR4, NF-κB, and Downstream Key Molecules in the Lung Tissue of Rats From the 3 Groups

Western blot results (Figure 5 and Figure 6) showed that, compared with the CG, the MG and IG exhibited significantly higher protein expression levels of TLR4, NF-κB p65, MyD88, and p-IκBα in lung tissue, while the expression of IκBα protein was significantly reduced (p<0.05). Compared with the MG, the IG showed a marked decrease in the protein expression of TLR4, NF-κB p65, MyD88, and p-IκBα and a significant increase in IκBα protein expression (p<0.05).

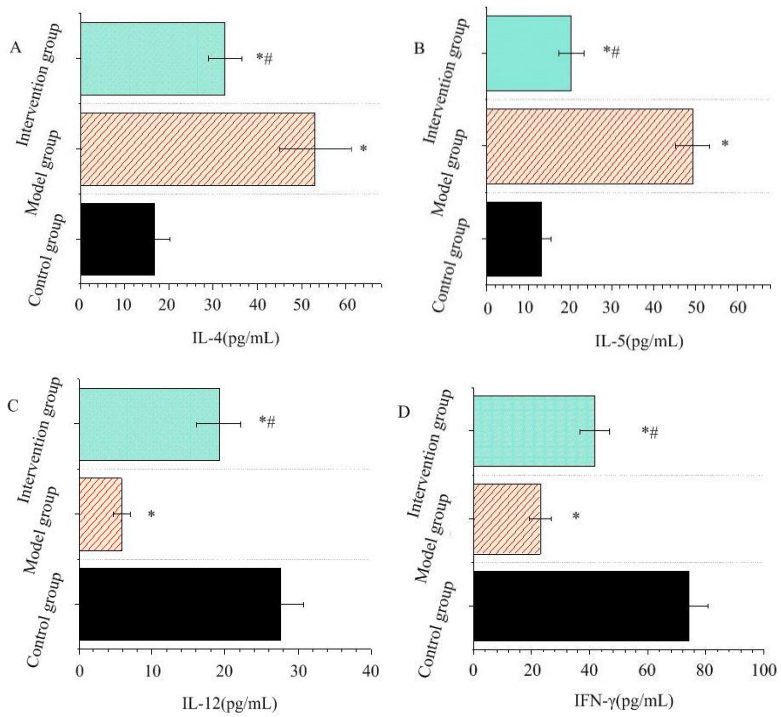

Figure 1. Comparison of T Helper 1/T Helper 2 (TH1/TH2) Cytokine Levels in Rat Bronchoalveolar Lavage Fluid (BALF). A. Levels of Interleukin-4 (IL-4). B. Levels of Interleukin-5 (IL-5). C. Levels of Interleukin-12 (IL-12). D. Levels of Interferon-γ (IFN-γ). Asterisk (*) indicates p<0.05 vs the control group (CG); number sign (#) indicates p<0.05 vs the model group (MG).

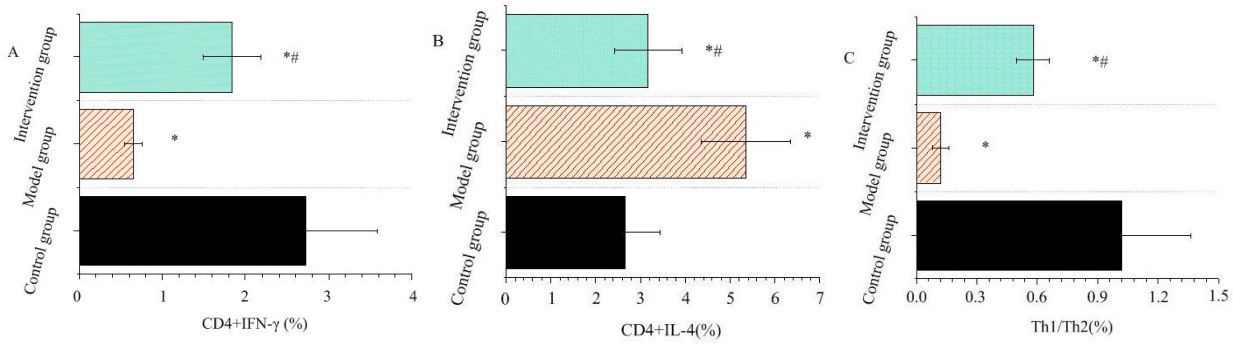

Figure 2. Comparison of T Helper 1/T Helper 2 (TH1/TH2) Cell Subpopulations in Rats. A. Proportions of CD4+Interferon-γ + (CD4+IFN-γ+) cells (TH1 cells). B. Proportions of CD4+Interleukin-4+ (CD4+IL-4+) cells (TH2 cells). C. The TH1/TH2 (T Helper 1/T Helper 2) ratio. Asterisk (*) indicates p<0.05 vs the control group (CG); number sign (#) indicates p<0.05 vs the model group (MG).

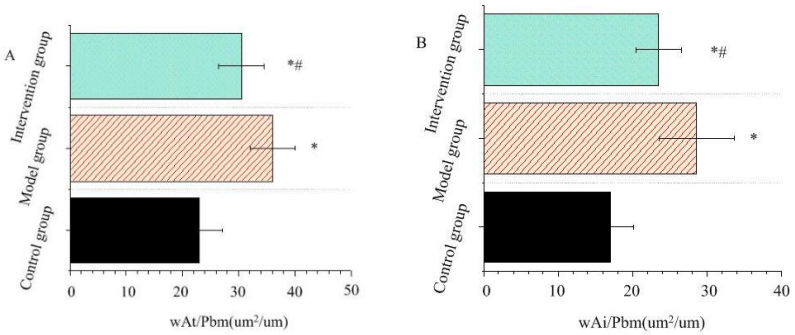

Figure 3. Comparison of Airway Remodeling (AR) Morphological Parameters wAt/Pbm (total wall area/bronchial basement membrane perimeter) and wAi/Pbm (inner wall area/bronchial basement membrane perimeter) in Rats. A. wAt/Pbm (total wall area/bronchial basement membrane perimeter). B. wAi/Pbm (inner wall area/bronchial basement membrane perimeter). Asterisk (*) indicates p<0.05 vs the control group (CG); number sign (#) indicates p<0.05 vs the model group (MG).

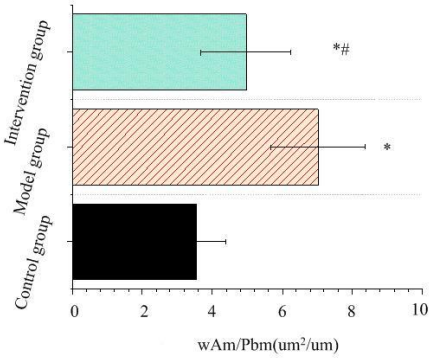

Figure 4. Comparison of Airway Remodeling (AR) Morphological Parameter wAm/Pbm (smooth muscle wall area/bronchial basement membrane perimeter) in Rats. Asterisk (*) indicates p<0.05 vs the control group (CG); number sign (#) indicates *p*<0.05 vs the model group (MG).

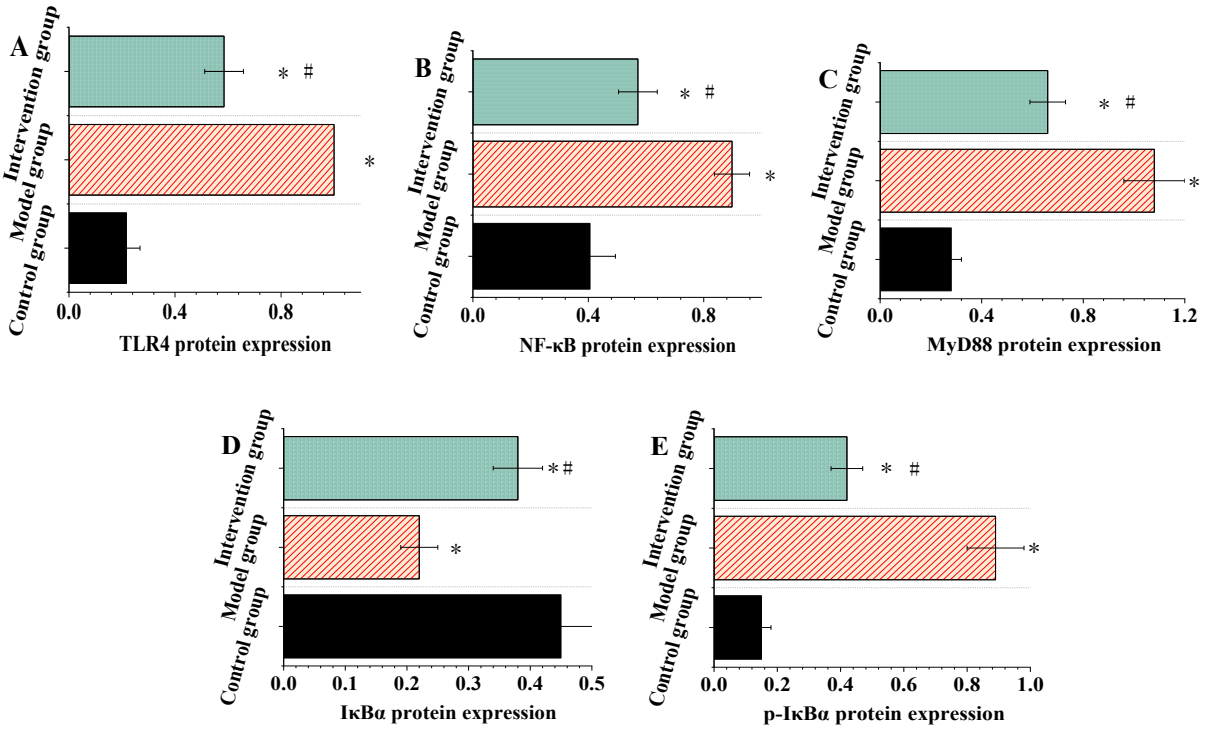

Figure 5. Comparison of Protein Expression of Toll-like Receptor 4 (TLR4), Nuclear Factor-κB (NF-κB), and Downstream Key Molecules (Myeloid Differentiation Primary Response 88 [MyD88], Inhibitor of NF-κBα [IκBα], phosphorylated IκBα [p-IκBα]) in the Lung Tissue of Rats From the 3 Groups (Control Group [CG], Model Group [MG], Intervention Group [IG]). A. TLR4 (Toll-like Receptor 4). B. NF-κB (Nuclear Factor-κB). C. MyD88 (Myeloid Differentiation Primary Response 88). D. IκBα (Inhibitor of NF-κBα). E. p-IκBα (phosphorylated IκBα). Asterisk (*) in dicates $p<0.05$ vs the control group (CG); number sign (#) indicates $p<0.05$ vs the model group (MG).

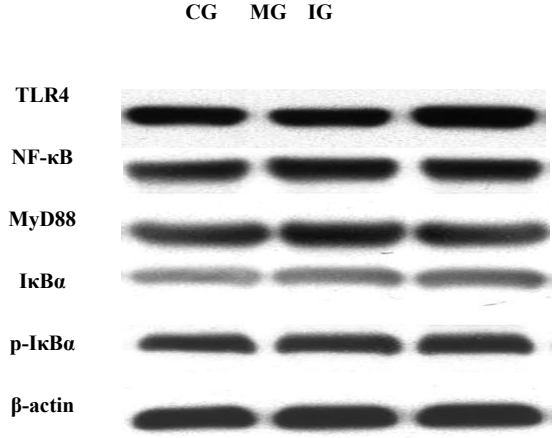

Figure 6. Western Blot (WB) Bands of Toll-like Receptor 4 (TLR4), Nuclear Factor-κB (NF-κB), and Downstream Key Molecules (Myeloid Differentiation Primary Response 88 [MyD88], Inhibitor of NF-κBα [IκBα], phosphorylated IκBα [p-IκBα]) in the Lung Tissue of Rats from the 3 Groups (Control Group [CG], Model Group [MG], Intervention Group [IG]). β-actin was used as the internal reference protein.

qPCR Gene Expression Analysis in the 3 Groups of Rats

qPCR results (Figure 7) showed that, compared with the CG, the MG exhibited a significant increase in the mRNA expression of *TLR4*, *MyD88*, and *NF-κB p65* in the lung tissue, while the mRNA expression of *IκBα* was significantly decreased (all $p<0.01$). Following intervention with a CB2 receptor inverse agonist, the IG exhibited the following changes compared with the MG: a significant downregulation in the mRNA expression of *TLR4*, *MyD88*, and *NF-κB p65* ($p<0.01$) and a significant upregulation of *IκBα* mRNA expression ($p<0.01$).

Comparison of the Asthma Induction Latent Period and tAAD Among the 3 Groups of Rats

As shown in Figure 8, compared with the CG, the latency to asthma induction was shorter and the tAAD was longer in both the MG and IG. Compared with the MG, the latency to asthma induction was longer and the tAAD was shorter in the IG ($p<0.05$ for all comparisons).

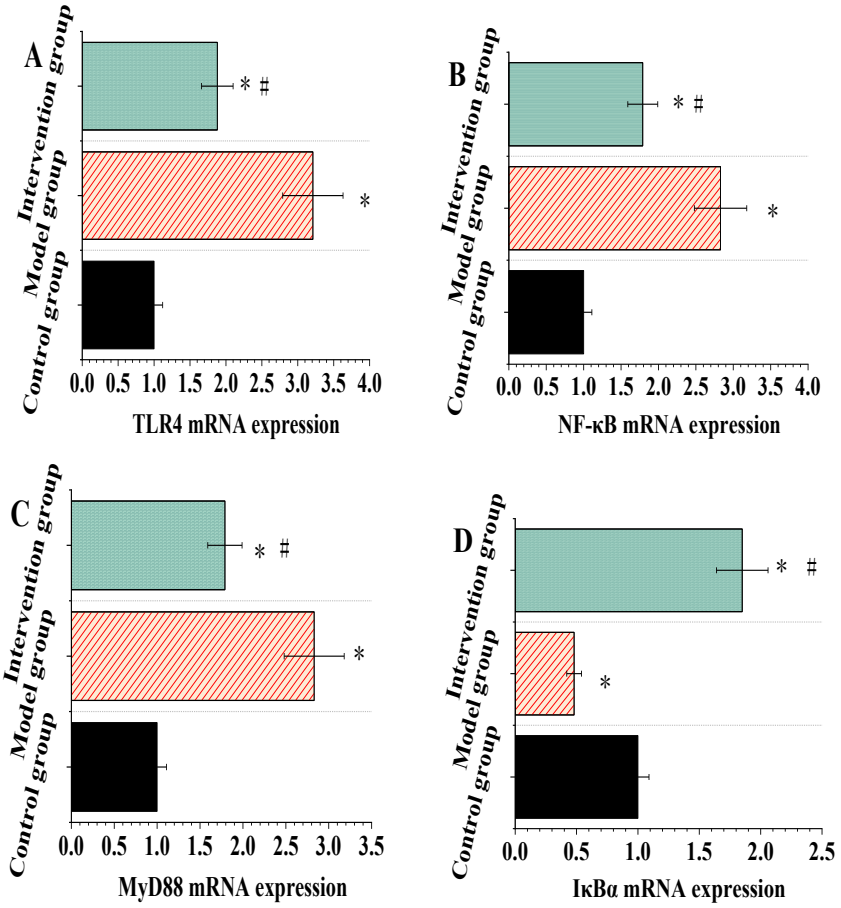

Figure 7. Quantitative Polymerase Chain Reaction (qPCR) Gene Expression Analysis in the 3 Groups of Rats (Control Group [CG], Model Group [MG], Intervention Group [IG]). A. Toll-like Receptor 4 (TLR4). B. Nuclear Factor-κB (NF-κB). C. Myeloid Differentiation Primary Response 88 (MyD88). D. Inhibitor of NF-κBα (IκBα). Asterisk (*) indicates p<0.05 vs the control group (CG); number sign (#) indicates p<0.05 vs the model group (MG).

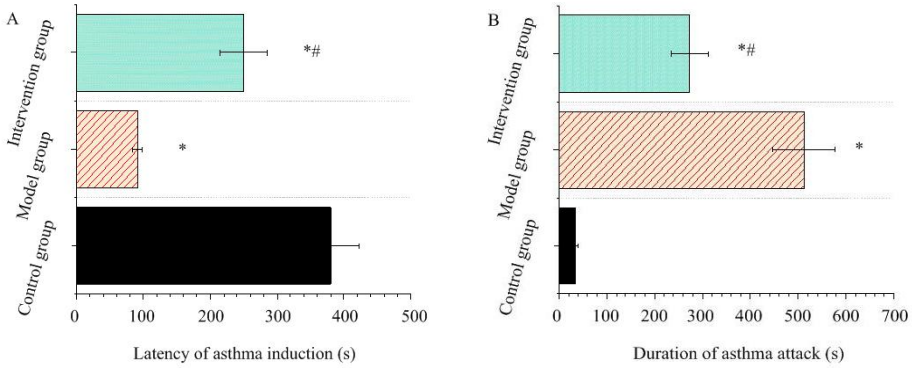

Figure 8. Comparison of the Latency to Asthma Induction and Total Asthma Attack Duration (tAAD) Among the 3 Groups of Rats. Note: The control group (CG) received physiological saline instead of OVA for sensitization/challenge and showed no asthma-like symptoms; its 'latency to asthma induction' was defined as the maximum observation duration (1800 seconds, 30-minute nebulization period) and 'tAAD' as 0 seconds. A. Latency to asthma induction (CG: 1800 seconds, no asthma response; MG/IG: measurable latency of asthma onset). B. Total asthma attack duration (tAAD; CG: 0 seconds, no attack; MG/IG: measurable attack duration). Asterisk (*) indicates p<0.05 vs the CG; number sign (#) indicates p<0.05 vs the model group (MG).

DISCUSSION

BA, as a complex and intractable chronic airway inflammatory disease, involves the imbalance of numerous cells and cytokine networks in its pathogenesis, with AR being a key factor leading to the persistence and deterioration of asthma and the continuous decline in lung function. [15]In recent years, the ECS, particularly the CB2 receptor, has garnered increasing attention for its potential role in immune regulation and inflammation control, thereby opening new avenues for asthma treatment research. This study focused on the CB2 receptor inverse agonist, and our findings collectively support a multi-step mechanism by which it exerts therapeutic effects on BA, with the TLR4/NF-κB pathway as a central mediator.[16]

First, the CB2 receptor inverse agonist rebalances the TH1/TH2 axis-a core driver of allergic airway inflammation in BA. In the OVA-induced asthma model, the shift toward TH2 dominance (elevated IL-4/IL-5, reduced IFN-γ/IL-12, and decreased CD4+IFN-γ+ cell proportion with increased CD4+IL-4+ cells) is consistent with the classic immunopathological feature of BA, where overactivated TH2 cells secrete pro-inflammatory cytokines to promote eosinophil infiltration and mucus hypersecretion. By restoring the TH1/TH2 equilibrium, the CB2 receptor inverse agonist likely interrupts this pro-inflammatory cascade: unlike conventional CB2 agonists that may induce tolerance with long-term use, its unique mode of stabilizing the inactive conformation of CB2 receptors may directly suppress TH2 polarization. [17,18]This could be achieved by regulating intracellular signal transduction, affecting the activity of transcription factors critical for TH2 differentiation, and guiding T lymphocytes to shift toward the TH1 direction, thereby reducing TH2-mediated inflammatory damage to the airways.[19]

Second, the CB2 receptor inverse agonist mitigates AR by targeting inflammation-driven airway structural changes. In the model group, long-term repeated OVA stimulation led to obvious airway wall thickening, as evidenced by increased wAt/Pbm, wAm/Pbm, and wAi/Pbm indices-changes that severely impair airway function and contribute to persistent asthma. After treatment with the CB2 receptor inverse agonist, these AR-related morphological parameters were significantly reduced in the intervention group, indicating the agonist's ability to inhibit the progression of AR. [20]The underlying mechanism is likely linked to its regulation of the TLR4/NF-κB pathway: by suppressing the activation of this pathway, the agonist may inhibit the infiltration and activation of inflammatory cells, block the transmission of inflammatory signals to airway structural cells (such as airway smooth muscle cells and fibroblasts), and thereby reduce smooth muscle cell proliferation, extracellular matrix deposition, and other biological processes associated with AR.[21]

Third, the CB2 receptor inverse agonist modulates the TLR4/NF-κB signaling pathway and its downstream key molecules, which serve as the molecular basis for its dual effects on immune balance and AR inhibition. In the model group, the upregulated protein and mRNA

expression of TLR4, NF-κB p65, MyD88, and p-IκBα, along with downregulated IκBα expression, confirmed the overactivation of the TLR4/NF-κB pathway in asthmatic lung tissue—this activation can amplify inflammatory responses and promote AR by regulating the expression of a large number of pro-inflammatory and pro-remodeling genes. After intervention with the CB2 receptor inverse agonist, the abnormal expression of these molecules was significantly reversed: TLR4, NF-κB p65, MyD88, and p-IκBα were downregulated, while IκBα was upregulated. This suggests the agonist inhibits TLR4/MyD88-dependent signaling, reduces IκBα phosphorylation and degradation, and blocks NF-κB activation-ultimately suppressing the downstream inflammatory and remodeling cascades.[22]

Notably, the improved functional outcomes (longer latency to asthma induction and shorter total asthma attack duration) in the intervention group further validate the therapeutic potential of the CB2 receptor inverse agonist. These changes reflect the integration of its effects on immune rebalancing and AR inhibition: by reducing airway inflammation and improving airway structural damage, the agonist decreases the sensitivity of the airways to asthma-inducing factors, prolongs the time to asthma onset, and shortens the duration of attacks-addressing both the acute symptomatic and chronic progressive aspects of BA.

Collectively, our results propose a clear therapeutic model for the CB2 receptor inverse agonist in BA: it suppresses the TLR4/MyD88/NF-κB pathway to achieve two key effects: (1) restoring TH1/TH2 immune homeostasis to alleviate allergic airway inflammation, and (2) inhibiting pro-remodeling signaling to reverse airway structural damage. This dual action addresses two core pathological hallmarks of BA, providing a more comprehensive intervention strategy compared to treatments that target only inflammation or remodeling in isolation.

This study focused on the effects of the CB2 receptor inverse agonist on BA. Through the construction of a rat model, it was found that the agonist has significant preventive and therapeutic potential, effectively regulating T_H1/T_H2 imbalance, inhibiting AR, and intervening in the pathological process of asthma through the TLR4/NF-κB pathway. However, it is important to note that this study is primarily based on animal models, and the feasibility of translating its results into clinical applications requires further validation. Additionally, due to experimental limitations, this study did not comprehensively assess the involvement of other potential signaling pathways or the long-term safety of the drug, factors that may influence the completeness of the study's conclusions. Future research should integrate multiomics analyses and preclinical toxicological evaluations to more fully elucidate the therapeutic potential and clinical applicability of the drug.

STATEMENT OF ETHICS

This study was reviewed and approved by the Animal Ethics Committee of Xi'an Qidi Children's Hospital (Approval No. XQCH051). All experimental procedures involving Sprague-Dawley (SD) rats strictly complied with the Guide for the Care and Use of Laboratory Animals (National Institutes of Health publication 80-23, revised 1978) and the 3Rs Principles (Replacement, Reduction, Refinement) for animal experimentation. Efforts were made to minimize animal suffering during the experiment.

FUNDING

This study received no specific grant from any funding agency in the public, commercial, or not-for-profit sectors. No external financial support was provided for the design of the study, collection, analysis, or interpretation of data, writing of the manuscript, or decision to submit the manuscript for publication.

CONFLICT OF INTEREST

The authors declare no competing interests.

ACKNOWLEDGMENTS

The authors would like to thank the staff of the Department of Respiratory Asthma and the Department of Integrated Traditional Chinese and Western Medicine at Xi'an Qidi Children's Hospital for their assistance in the implementation of the animal experiment and sample collection process. Gratitude is also extended to the laboratory technicians who provided support for the detection of cytokines, flow cytometry analysis, and Western blot experiments, ensuring the smooth progress of the study.

DATA AVAILABILITY

The raw and processed data supporting the findings of this study are available upon reasonable request from

the corresponding author, Wen Zhou (Department of Respiratory Asthma, Xi'an Qidi Children's Hospital, Xi'an, Shaanxi, China). Requests can be submitted via email at: 15101277712@163.com. All data will be provided in compliance with academic research ethics and the data management regulations of Xi'an Qidi Children's Hospital to ensure the integrity and confidentiality of experimental information.

AI ASSISTANCE DISCLOSURE

No artificial intelligence (AI) tools, including butnot limited to AI-powered writing assistants, data analysis software with AI functions, or AI-based image processing tools, were used in any stage of preparing this manuscript—including experimental design, data collection, statistical analysis, manuscript drafting, revision, or figure preparation. All content and data presented in this study are the result of independent experimental work and manual analysis by the authors.

REFERENCES

1. Qian K, Xu H, Chen Z, Zheng Y. Advances in pulmonary rehabilitation for children with bronchial asthma. Zhejiang Da Xue Xue Bao Yi Xue Ban. 2023;52(4):518–25.
2. Chetta A, Calzetta L. Bronchial asthma: an update. Minerva Med. 2022;113(1):1–3.
3. Savin IA, Zenkova MA, Sen'kova AV. Bronchial asthma, airway remodeling, and lung fibrosis as successive steps of one process. Int J Mol Sci. 2023;24(22):16042.
4. Kama Y, Yamada Y, Koike T, Suzuki K, Enseki M, Hirai K, et al. Antibiotic treatments prolong the wheezing period in acute exacerbation of childhood bronchial asthma. Int Arch Allergy Immunol. 2022;183(6):617–27.
5. Liu H, Tang T. MAPK signaling pathway-based glioma subtypes, machine-learning risk model, and key hub proteins identification. Sci Rep. 2023;13(1):19055.
6. Britt RD Jr, Ruwanpathirana A, Ford ML, Lewis BW. Macrophages orchestrate airway inflammation, remodeling, and resolution in asthma. Int J Mol Sci. 2023;24(13):10451.
7. Liu H, Li Y. Potential roles of cornichon family AMPA receptor auxiliary protein 4 (CNIH4) in head and neck squamous cell carcinoma. Cancer Biomark. 2022;35(4):439–50.
8. Garagorri-Gutiérrez D, Leirós-Rodríguez R. Effects of physiotherapy treatment in patients with bronchial asthma: A systematic review. Physiother Theory Pract. 2022;38(4):493–503.
9. Thomas D, McDonald VM, Pavord ID, Gibson PG. Asthma remission: what is it and how can it be achieved? Eur Respir J. 2022;60(5):2102583.
10. Chung KF, Dixey P, Abubakar-Waziri H, Bhavsar P, Patel PH, Guo S, et al. Characteristics, phenotypes, mechanisms, and management of severe asthma. Chin Med J (Engl). 2022;135(10):1141–55.
11. Fong KY, Zhao JJ, Syn NL, Nair P, Chan YH, Lee P. Comparing bronchial thermoplasty with biologicals for severe asthma: Systematic review and network meta-analysis. Respir Med. 2023;216:107302.
12. Matucci A, Micheletto C, Vultaggio A. Severe asthma and biologics: managing complex patients. J InvestigAllergol Clin Immunol. 2023;33(3):168–78.
13. Rajvanshi N, Kumar P, Goyal JP. Global initiative for asthma guidelines 2024: an update. Indian Pediatr. 2024;61(8):781–6.
14. Dhangar S, Shanmukhaiah C, Sawant L, Ghatanatti J, Shah A, Mathan SLP, et al. Synergetic effect of azacitidine and sorafenib in treatment of a case of myeloid neoplasm with sole chromosomal abnormality t(8;22)(p11.2;q11.2)/BCR-FGFR1 rearrangement. Cancer Genet. 2023;274–5:26–9.
15. Barosova R, Baranovicova E, Hanusrichterova J, Mokra D. Metabolomics in animal models of bronchial asthma and its translational importance for clinics. Int J Mol Sci. 2023;25(1):459.
16. Li C, Xin H, Yun L, BoWen L, KunLu S, JiangTao L. Bronchial thermoplasty for severe asthma: potential mechanisms and response markers. Ther Adv Respir Dis. 2024;18:17534666241266348.
17. Leung C, Sin DD. Asthma-COPD overlap: what are the important questions? Chest. 2022;161(2):330–44.
18. Dai Y, Jin N. Association and interacting factors between bronchial asthma and attention-deficit hyperactivity disorder in children: meta-analysis and systematic review. Actas Esp Psiquiatr. 2023;51(6):262–70.
19. Habib N, Pasha MA, Tang DD. Current understanding of asthma pathogenesis and biomarkers. Cells. 2022;11(17):2764.
20. Amison RT, Page CP. Novel pharmacological therapies for the treatment of bronchial asthma. Minerva Med. 2022;113(1):31–50.
21. Ano S, Kikuchi N, Matsuyama M, Hizawa N. Patient profiling to predict response to bronchial thermoplasty in patients with severe asthma. Respir Investig. 2023;61(6):675–81.
22. Nakagome K, Nagata M. The possible roles of IL-4/IL-13 in the development of eosinophil-predominant severe asthma. Biomolecules. 2024;14(5):546.